УДК 539.172.17, 539.17.012

PRODUCTION OF HEAVY EVAPORATION RESIDUES IN THE REACTIONS INDUCED BY AN EXTRACTED ^{48}Ca BEAM ON A ^{208}Pb TARGET

A.V.Yeremin, V.I.Chepigin, M.G.Itkis, A.P.Kabachenko, S.P.Korotkov, O.N.Malyshev, Yu.Ts.Oganessian, A.G.Popeko, J.Rohác, R.N.Sagaidak, M.L.Chelnokov, V.A.Gorshkov, A.Yu.Lavrentev, S.Hofmann[1], G.Münzenberg[1], M.Veselsky[2], S.Sharo[3], K.Morita[4], N.Iwasa[4], S.I.Mulgin[5], S.V.Zhdanov[5]

The production cross sections of the isotopes $^{253-255}$No were measured for the heavy ion complete fusion reaction ^{48}Ca + ^{208}Pb using the electrostatic recoil separator VASSILISSA. The obtained excitation functions for the reaction products formed after the evaporation of 1–3 neutrons from the compound nucleus are discussed and compared with the data obtained earlier and with the results of the statistical model calculations. The background conditions at the extraction of the correlated events of the reaction product decay are also considered from the point of view of future experiments on the superheavy element synthesis in the complete fusion reactions induced by ^{48}Ca projectiles.

The investigation has been performed at the Flerov Laboratory of Nuclear Reactions, JINR.

Получение тяжелых ядер остатков испарения в реакциях на выведенном пучке ^{48}Ca на мишени ^{208}Pb

А.В.Еремин и др.

Сечения образования изотопов $^{253-255}$No были измерены в реакции полного слияния ^{48}Ca + ^{208}Pb с использованием электростатического сепаратора ядер отдачи ВАСИЛИСА. Обсуждаются полученные функции возбуждения продуктов реакций, образованных после испарения 1-3 нейтронов из компаунд-ядра, и проводится сравнение с данными, полученными ранее, и с результатами расчета по статистической модели. Рассматриваются фоновые условия при извлечении коррелированных событий распада продуктов реакций с точки зрения будущих экспериментов по синтезу сверхтяжелых элементов в реакциях полного слияния под действием налетающих частиц ^{48}Ca.

Работа выполнена в Лаборатории ядерных реакций им. Г.Н.Флерова ОИЯИ.

[1]Gesellschaft für Schwerionenforschung, D-64220 Darmstadt, Germany
[2]Institute of Physics, SK-84228 Dubravska 9, Bratislava, Slovakia
[3]Comenius University, Bratislava, Slovakia
[4]Institute of Physical and Chemical Research (RIKEN), Wako-shi, Saitama 351-01, Japan
[5]Institute of Nuclear Physics, National Nuclear Centre, 480082 Almaty, Republic of Kazakhstan

1. Introduction

The use of ^{48}Ca ions as projectiles in production of the heaviest elements is of special interest. Their neutron-excess makes it possible to gain access to compound nuclei (CN) whose neutron numbers are close to the predicted magic neutron numbers $N = 178–184$ [1]. The doubly magic structure ($Z = 20$, $N = 28$) of ^{48}Ca allows one to form relatively cold CN at energies close to the fusion barrier and to hope that the fusion hindrance observed in heavy systems [2,3] might be reduced owing to the shell structure of this nuclide as it is observed in the reactions induced by the ^{86}Kr ($N = 50$) projectile [4]. All these reasons are discussed once again within the framework of the proposal to use the reactions ^{48}Ca + ^{232}Th, ^{238}U, ^{242,244}Pu, as the most promising ones, in production of the heaviest isotopes of the elements with $Z = 110–114$ [5]. Earlier, attempts to synthesize the elements with $Z = 110–116$ in the complete fusion reactions induced by ^{48}Ca ended in negative results [6–9].

At the end of 1997 an intensive external beam of ^{48}Ca was obtained at the U-400 cyclotron of the FLNR (JINR) after installation and putting into operation an ECR ion source [10]. It opened new prospects for the search for the heaviest elements with the use of the modern electrostatic recoil separator VASSILISSA [11] installed at the beam line of U-400. Some improvements of the detector module of the separator VASSILISSA alongside with the available beam of ^{48}Ca enabled us to carry out experiments on the synthesis of the heaviest elements ($Z \geq 110$) within a reasonable beam time or to achieve the upper limit value of several pb for the production cross section of evaporation residues (ER) in a 30-40 day irradiation. Earlier, using this set-up [12], the asymmetric or the so-called «hot» fusion reactions leading to Fm, No, and Db isotopes were investigated using ^{20,22}Ne, ^{26}Mg, ^{27}Al, and ^{31}P projectiles and actinide targets. The analysis of the measured production cross sections for the observed evaporation residues did not reveal any evidence for existing a hindrance to fusion at an ion bombarding energy in the vicinity of the fusion barrier. Excitation energies of the CN in these studies were in the range from 40 to 60 MeV.

The aim of the present work was a comprehensive test of the ion source, the U-400 cyclotron and separator performances in long-term experiments with an intensive beam aimed at the synthesis of the heaviest elements today and in the nearest future. For this purpose we chose the reactions ^{208}Pb(^{48}Ca, xn) as test reactions. The excitation functions for the ^{208}Pb(^{48}Ca, $1n - 3n$) reactions were earlier measured in detail [13]. Rather good agreement of the results of these measurements with the data obtained earlier (see, for instance, the compilation in [14]) was obtained. The reaction kinematics and decay modes of the ER allow one to consider this choice as a good testing on the way to the synthesis of the heaviest elements. In the course of the present work we also attempted to obtain new data on the ^{208}Pb(^{48}Ca, γ) and ^{208}Pb(^{48}Ca, $4n$) reactions and considered deexcitation of the compound nucleus within the framework of statistical model approximations. In our study, keeping in mind future experiments, we paid special attention to the background conditions which could interfere with the events searched for.

2. Experiment

An external ^{48}Ca beam was obtained with the use of a new ECR-ion source ECR-4M, installed at the U-400 cyclotron and coupled with the external injection line delivering primary ions to the central region of the cyclotron. A ^{48}Ca material enriched to 70% was used for feeding the ion source in the experiments. This material was prepared as a mixture of CaO and Al powder and placed into a crucible heated up to 1100 K. The average consumption of the material in the ECR source was 0.3 mg/h at the beam intensity on the target of $(5-7)\times 10^{11}$ s^{-1}. In the experiments, the continuous beam mode was used.

The beam energy was controlled by measuring the energy of the ions scattered at 30° in a thin gold foil. The energies of the ^{48}Ca beams extracted from U-400 were 220, 245 and 255 MeV. Carbon foils installed in front of the scattering gold foil were used as degraders to vary smoothly the beam energy. The measured energy spread of the scattered ions was in the range of (1.5–2.5)% (FWHM).

The ^{208}Pb target was prepared by means of evaporation of a metal onto a 1.54 mg/cm^2 aluminium backing disk 120 mm in diameter. The disk was used as a self-supporting rotating target wheel. The thickness of the target was equal to 0.19 mg/cm^2 of ^{208}Pb enriched to 98.2%.

The projectile energy in the half-thickness of the target (E_{lab}) was calculated using the measured value for the scattered ions and taking into account energy losses in the target backing and in the half thickness of the target. The energy losses were computed with the SRIM-97 code [15].

The produced ER were separated in-flight by the electrostatic recoil separator VASSILISSA [11,12]. The registration system had been considerably modernized in respect of the detector and data acquisition systems. The detector system consisting of two (start and stop) time-of-flight (TOF) detectors [16] had been improved and installed in the separator focal plane. The value of 99.95% had been achieved for the detection probability of heavy ER by making use of a single timing detector. After passing the TOF detectors, the recoil nuclei were implanted into a position-sensitive detector array which consisted of 16 silicon strips. The active area of the silicon strip detector was 60×60 mm^2. Each strip was position sensitive in the vertical direction with a relative resolution of 0.65 mm for the α decay of a decay chain. The strip detector was surrounded by other four identical silicon backward detectors and the entire array had a shape of a cube with the dimensions $60\times 60\times 60$ mm^3. The geometrical efficiency of the silicon array was 85% of 4π. In the described experiments backward detectors were not used. A schematic view of the separator and its detection system is presented in Fig.1.

The energy resolution of the array was about 25 keV in the summed spectrum (composed of all the strips) for the α particles collected in an energy range from 6 to 10 MeV. The spectrometric system was preliminary calibrated with external spectrometric α sources. The final calibration was performed with the test reaction ^{48}Ca + ^{174}Yb leading to production of Th isotopes and their daughter products at different projectile energies. These products give the well-known α lines in the searched region of α energy. From the studies of the test reactions ^{48}Ca + ^{159}Tb, ^{174}Yb we came to a conclusion that a 3–4 μm mylar degrader foil placed in front of the silicon detectors essentially improves the background conditions for the implanted α-activity measurements.

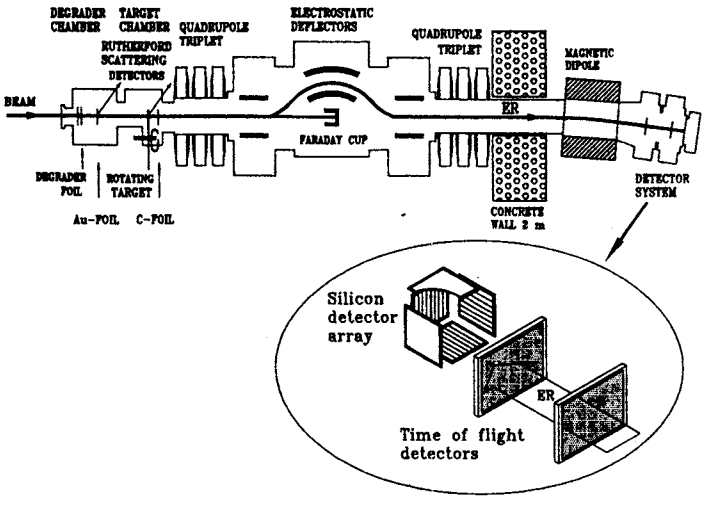

Fig. 1. Schematic view of the separator and detection system. The main components of the set-up are designated in the figure

The signals from the TOF detectors were used to distinguish impinged events (recoil or scattered particles) from α decay of the implanted products. Owing to the high efficiency of the TOF-system [16], the very clean decay α spectra of the searched products could be obtained. That circumstance had to be checked under conditions of continuous beam irradiation. The low background in α spectra is very important especially when searching for the correlated events for the decays $^{254}\mathrm{No} \xrightarrow[8.09\ \mathrm{MeV}]{55\ \mathrm{s}} {}^{250}\mathrm{Fm} \xrightarrow[7.43\ \mathrm{MeV}]{30\ \mathrm{m}} {}^{246}\mathrm{Cf}$, being the main activities produced in the $^{208}\mathrm{Pb}(^{48}\mathrm{Ca}, 2n)$ reaction. The time window for the correlated events of the daughter decays has to be a few hours in that case.

The data acquisition system of VASSILISSA allows one storage of information in a list mode manner about energy, position, TOF and arrival time of the recoil nuclei implanted into the focal plane detector, as well as position, detecting time and energy of alpha decays and spontaneous fission events in the detectors. The accuracy of the time determination for all the events is equal to 1 μsec. The analog input signals are digitized and transformed into events by the CAMAC electronics occupying 3 CAMAC crates. A specially developed interface was installed to transfer the data from the CAMAC crates by means of a DMA-channel to a PC-486 located in the detector room of the separator. That PC collected the events and sent them in blocks through a 100 Mbit/s Fast Ethernet to another PC installed in the control room. The last-mentioned PC supervised the system and stored the data.

The acquired data were then made available to a DEC Alpha Station running GOOSY environment [18] part of which was a specially written code [19] executing the analysis. The code could be controlled by a large set of parameters making it flexible in the sence of data processing which included the calibration of event parameters, accumulation of various spectra and looking for chains of correlated events.

To estimate transmission of the separator, a Monte-Carlo computer code was developed [17]. The code takes into account the emittance of the projectile beam, the reaction kinematics including the momentum transfer to the ER from the light particles (n, p and α) evaporated from CN, the multiple scattering and energy losses of ER in the target and foils and the ionic charge distribution of ER. The code generates «real» particles and puts them through the separator, from element to element, using first-order ion optics.

The transmission value of the separator was checked for the ER produced in a test reaction induced on a ^{159}Tb target. The value was derived by comparison of the yield of the ER implanted into the focal plane detector and that measured at a catcher foil placed right behind the target. The ^{201}At nuclei ($T_{1/2} = 1.5$ m, $E_\alpha = 6.34$ MeV) were a main product of the (^{48}Ca, $6n$) reaction at the energy $E_{lab} = 220$ MeV. The measured value of the transmission for the test reaction was in good agreement with the value obtained as a result of simulations (difference between the absolute values did not exceed more than 20 %).

The optimal separator's setting for the ^{208}Pb(^{48}Ca, xn) reactions under investigation was based on a simulation [17] performed for the reaction ^{208}Pb(^{48}Ca, $2n$) and sufficient suppression of low-energy beam-like particles (see below) as it was deduced from the measurements with the beam and lead target. The values of the transmission corresponding to the optimal separator's setting were in the range from 44% to 42% at the projectile energies corresponding to the maxima of the excitation functions for the $1n$ to $3n$ reaction channels.

As a result of the overall improvement, the flow of low energy beam-like particles passing through the TOF-system was suppressed by a factor of ~ 10^{10} in comparison with the beam intensity at the target. The count rate at the stop detector array was reduced by an additional factor of 10 owing to the partial absorption of the particles in the TOF detector foils and in the degrader foils installed in front of the stop detectors. The measurements of the recoil energy and TOF allowed us to suppress additionally that background within the factor of ~ 100. The overall background suppression of the low-energy beam-like particles as high as 10^{13} was achieved mainly depending on the tuning of U-400.

3. Results

3.1. Excitation Functions for the ^{208}Pb(^{48}Ca, xn) *Reaction Products.* Formation of the $^{252-256}$No isotopes was studied within the projectile energy range of 204–235 MeV. The decay properties of these isotopes and their daughter products are well-known [20]. New data on the properties of ^{253}No were obtained recently [21].

Note that the decay properties of most mother → daughter → grand-daughter products are not completely suitable (with the exception of the chain $^{252}\text{No} \xrightarrow[8.42\ \text{MeV}]{2.3\ \text{s}} {}^{248}\text{Fm} \xrightarrow[7.87\ \text{MeV}]{36\ \text{s}} {}^{244}\text{Cf} \xrightarrow[7.21\ \text{MeV}]{19.4\ \text{m}} {}^{240}\text{Cm}$) for the use of correlation analysis methods (delayed α coincidences). The mother products (^{253,255}No) have complex spectra of α particles [20,21] with the most intensive lines close to the main α line of ^{254}No ($E_\alpha = 8.093$ MeV) produced in the ^{208}Pb(^{48}Ca, $2n$) reaction. Only this activity was observed in previous experiments [23, 24]. On the other hand the α energy of the observed

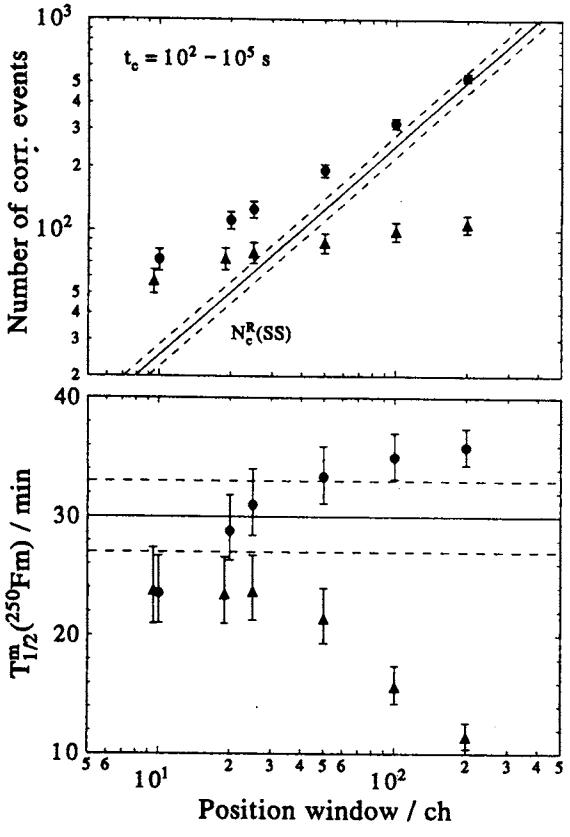

Fig. 2. The influence of the position window width on the number of the correlated events (upper panel) and the obtained half-life value for the daughter nucleus (bottom panel). The filled circles are related to the «all possible» correlations, whereas the filled triangles — to the «first found» ones. The solid line at the upper panel shows the level of random correlations deduced from the single spectrum, $N_c^R(SS)$, with the corresponding error corridor (the dashed lines). The solid line in the bottom panel shows the tabulated half-life value for ^{250}Fm with the corresponding uncertainties (the dashed lines). For further details see the text

activity is very close to the activity of ^{213}Rn ($E_\alpha = 8.088$ MeV), which could be produced in transfer reactions as it follows from the previous observations in the reactions induced by ^{40}Ar and ^{50}Ti on Pb targets [25,26]. The same situation is observed for the daughter product of the $2n$ evaporation reaction channel. The energy of α decay of ^{250}Fm ($E_\alpha = 7.430$ MeV) could interfere with the main α line of ^{211}Po ($E_\alpha = 7.450$ MeV) produced in the transfer reactions [25, 26]. As for the other daughter products, from our previous measurement [22], the established α-branch fraction for ^{249}Fm (the daughter product of the $3n$ reaction channel) was $(32.8 \pm 8.5)\%$ (compared with the value of 15% from systematics [20]). For ^{251}Fm (the daughter product of the $1n$ reaction channel) the α-branch fraction is only $(1.80 \pm 0.13)\%$ [20].

The methods of $\alpha - \alpha$ correlation analysis were applied to extract the data on the cross section values for the $2n$ evaporation channel. At first, to choose the correct set of parameters defining the correlated mother-daughter event in our data processing program, we fixed the ranges of α energy for the mother ($E_{\alpha 1} = 7.95$–8.25 MeV) and daughter ($E_{\alpha 2} = 7.30$–7.60 MeV) nuclei and looked for correlations within the decay time of the daughter nucleus ($t_c = 10^2 - 10^5$ s), varying the width of the position window. In Fig. 2 the results of these studies for the number of the correlated events (upper panel) and the deduced value of the half-life for the daughter nucleus (bottom panel) are shown for the data accumulated at $E_{lab} = (222.6 \pm 2.7)$ MeV. We searched for «all possible» mother-daughter correlations and the «first found» ones permitted by the chosen set of parameters.

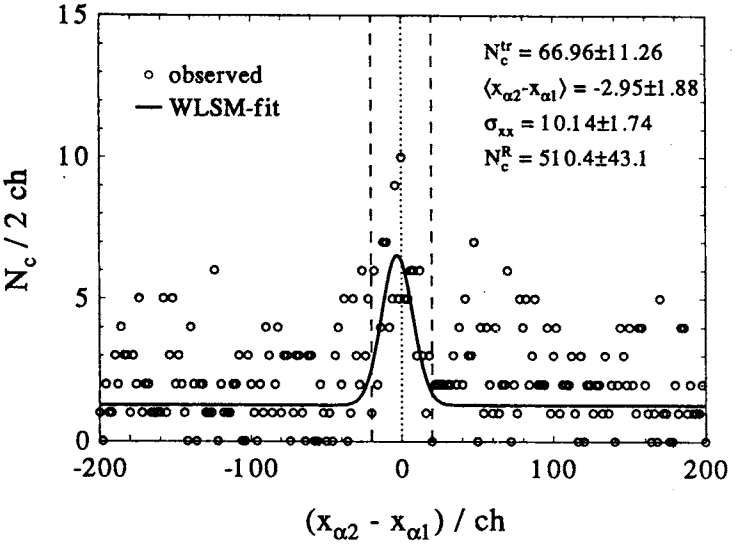

Fig. 3. The spectrum of displacements in the positions of the mother ($x_{\alpha 1}$) and daughter ($x_{\alpha 2}$) correlated events, N_c. The correlation parameters are the same as in Fig. 1. The solid line is the result of the gaussian plus constant background function fit obtained by the weighted least square method (WLSM). The results of the fit are shown in the upper right corner of the figure. The dashed lines indicate the position window corridor (± 20 ch) to which spectra shown in Fig.3 correspond to. For further details see the text

As is seen from the figure, good agreement of the measured half-life, $T^m_{1/2}$ obtained by the maximum likelihood method [27], with the tabulated data [20] for the daughter nucleus was obtained for «all possible» correlations at the position window width of $\pm 20 - 25$ channels (maximum width of 900 channels is equivalent to the length of a strip). The obtained numbers of the correlated events for different position windows, N_c are compared (in the figure) with the numbers of random correlated events, $N^R_c(SS)$, which could be estimated from the single spectrum. The obtained values of the true correlations, $N^{tr}_c = N_c - N^R_c(SS)$, are about the same and in good agreement with the value extracted from the correlated spectrum of the displacements in the mother-daughter positions, $(x_{\alpha 2} - x_{\alpha 1})$, as is shown in Fig.3. In this figure the numbers of correlated events (N_c) were fitted by the weighted least square method (WLSM) with a composition of gaussian and constant background functions corresponding to the true (N^{tr}_c) and random correlations (N^R_c), respectively. This approach was applied to the data obtained at each bombarding energy to estimate the number of events determining the values of the cross sections for the $2n$ evaporation channel.

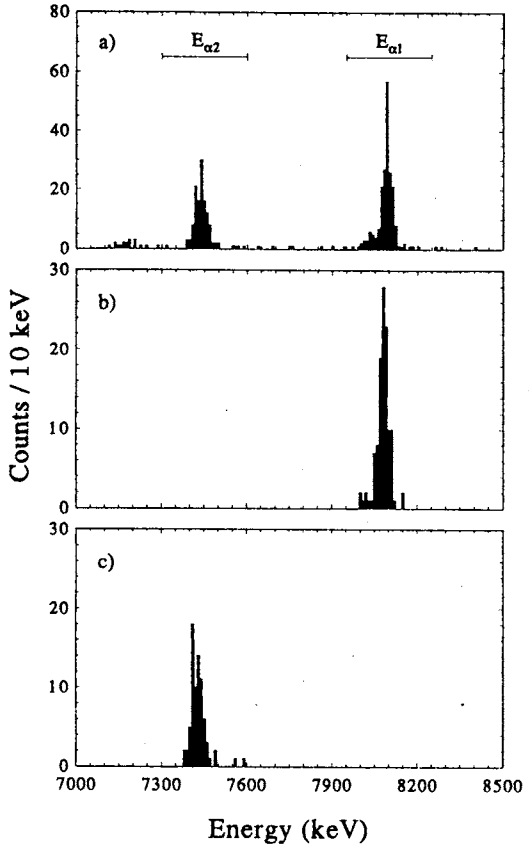

Fig. 4. The α spectra of the reaction products obtained at the 223 MeV beam energy: *a* — the single spectrum; *b* — the first α particle correlated to the second one; *c* — the second α particle correlated to the first one. The ranges of energies for the first and second α particles are designated in the upper panel of the figure. For further details see the text

In Fig.4*a*, an example of the single spectrum collected at E_{lab} =222.6± ±2.7 MeV is shown. In the α-energy range of 7.0–8.5 MeV two main groups in the vicinity of 7.45 and 8.1 MeV were observed at each of the bombarding energies. In Fig.4, in addition to the single spectrum (Fig.4*a*), the spectra of the first (in time) α particles correlated with the second ones (Fig.4*b*) and the second (in time) α particles correlated with the first ones (Fig.4*c*) are presented. The chosen width of the position window was ±20 channels whereas the t_c and $E_{\alpha 1,2}$ values were the same as it was mentioned above and used in Figs.2,3.

The obtained energy dependence for the ^{208}Pb(^{48}Ca, 2*n*) reaction cross section is shown in the upper panel of Fig.5.

The cross section values for the 1*n* and 3*n* evaporation channels were estimated basing on the single α spectra and using data on α energies for ^{255}No [20] and ^{253}No [21]. The obtained cross section values are shown in the middle panel of Fig.5. Only the upper limits for the cross section values were obtained for the 1*n* channel at the lowest bombarding energy and for the 1*n* and 3*n* channels at E_{lab} = (216.2 ± 1.4) MeV. Since no additional information on the identification of the α groups assigned to the considered nuclei was available, these data have only a tentative character. We estimate the relative accuracy of these data within ±50% in addition to the statistical error shown in the figure.

At the highest bombarding energy we searched for the ^{208}Pb(^{48}Ca, 4*n*)^{252}No reaction. We did not find either correlations in the chain $^{252}\text{No} \xrightarrow[8.42\ \text{MeV}]{2.3\ \text{s}} {}^{248}\text{Fm} \xrightarrow[7.87\ \text{MeV}]{36\ \text{s}} {}^{244}\text{Cf} \xrightarrow[7.21\ \text{MeV}]{19.4\ \text{m}} {}^{240}\text{Cm}$ or any events in the vicinity of the 8.42 MeV α energy (the most intensive α line of ^{252}No) in the single spectrum. From this non-observation we estimated the upper limit for the cross section value. It proved to be 3 nb at E_{lab} = (233.7 ± 1.8) MeV.

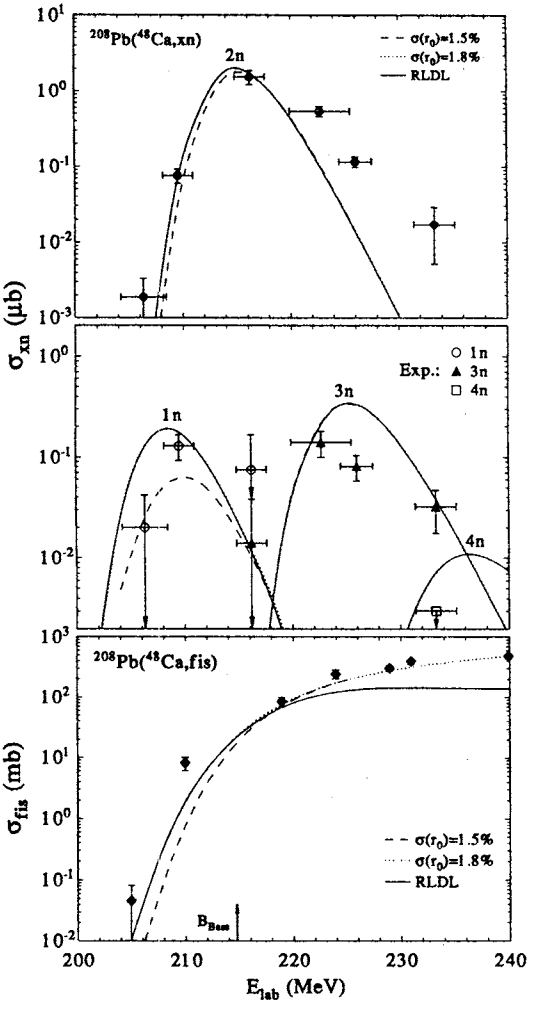

Fig. 5. The excitation functions for the ^{208}Pb(^{48}Ca, xn) and ^{208}Pb(^{48}Ca, fis) reactions. The upper panel — the results of measurements based on mother-daughter correlation analysis for the $2n$ evaporation channel. The middle panel — the results based on the single spectra analysis for the $1n$, $3n$ and $4n$ evaporation channels. The bottom panel — the results of the fission cross section measurement. The results of calculations using the HIVAP-code are designated by different lines. For further details see the text

We searched for the radiative capture reaction ^{208}Pb(^{48}Ca, γ)^{256}No at the lowest bombarding energy corresponding to the maximum of the excitation function for this reaction according to our estimations. A beam dose of 2.3×10^{16} was deposited within 15 hours of the target irradiation. During this time and 79 hours of the counting time after the end of the irradiation we attempted to observe the events corresponding to the decay chain

$$^{256}\text{No} \xrightarrow[8.45\ \text{MeV}]{2.9\ \text{s}} {}^{252}\text{Fm} \xrightarrow[7.04\ \text{MeV}]{25.4\ \text{h}} {}^{248}\text{Cf}.$$

From these measurements only the upper limit for the cross section for the ^{208}Pb(^{48}Ca, γ)^{256}No reaction was derived. It proved to be 1 nb at $E_{lab} = (206.3 \pm 2.1)$ MeV.

3.2. Transfer reactions. At the highest bombarding energies, direct production of ^{211}At as a result of the $+3p$ transfer from the projectile to the target nucleus (here and below we mean the minimal number of transferred nucleons) was clearly observed as it followed from the analysis of the single spectra, i.e., the ratio between the α activities of ^{211}At ($E_\alpha = 5.87$ MeV) and its EC-daughter ^{211}Po ($E_\alpha = 7.45$ MeV) corresponded to the tabulated values for their α- and EC-branch fractions [20]. At lower energies the production yield of ^{211}At decreases sharply, whereas the yield of the observed composite 7.43 and 7.45 MeV activity is increased. Thus, we could only estimate the yield of ^{211}Po, as a result of the $+2p+n$ transfer to the target nucleus, by means of comparing the counts in the single spectra and the results of the correlation analysis for the $^{254}\text{No} \xrightarrow[8.09\ \text{MeV}]{55\ \text{s}} {}^{250}\text{Fm} \xrightarrow[7.43\ \text{MeV}]{30\ \text{m}} {}^{246}\text{Cf}$ decay. In the same manner we

estimated the yield of ^{213}Rn ($E_\alpha = 8.09$ MeV), as a result of the $+4p+n$ transfer to the target nucleus. Keeping in mind a strong difference between the kinematics of heavy transfer products and ER [29] as well as different dependence of their yields on the bombarding energy in the vicinity of the Coulomb barrier [30], the absolute values for the production cross sections are questionable because of the tuning of the separator to the optimal transmission of the ER formed in the complete fusion reactions. The values of the observed cross sections corresponding to the 100% transmission for the transfer products are in the range from 0.01 μb to 1 μb for the energy range $E_{lab} = 206$–233 MeV studied in the present work.

From the observed upper limits of the cross section values for transfers we could estimate the suppression factors of the separator for those transfer reaction products whose absolute production cross sections were earlier measured [23]. For ^{211}Bi, ^{211m}Po and ^{212m}Po the obtained values of the suppression factor are increased from $> 10^2$ at the lowest bombarding energy to $> 10^4$ at the highest bombarding energy as a result of a growth of the absolute production cross sections and preferred forward peaking of heavy transfers at sub-barrier projectile energies.

4. Discussion

The unambiguous identification of the correlated events assigned to the pair $^{254}\text{No} \rightarrow {}^{250}\text{Fm}$ allows one to compare the excitation function obtained in the present work for the $^{208}\text{Pb}(^{48}\text{Ca}, 2n)^{254}\text{No}$ reaction with the previuos data [13,23] and calculations. The differences between the present measurements and the previous data [13] are not significant as it follows from the gaussian fit to both measurements and subsequent analysis of the data. Agreement of our excitation functions for the $1n$ and $3n$ reaction channels with those of [13] is quite satisfactory, keeping in mind the problems of the identification, as it was mentioned above. The cross section limit derived for the $^{208}\text{Pb}(^{48}\text{Ca}, \gamma)^{256}\text{No}$ reaction (1 nb) is comparable with the data [31] obtained earlier for the $^{204}\text{Pb}(^{48}\text{Ca}, \gamma)^{252}\text{No}$ reaction (0.5 nb), whereas our limit for the $^{208}\text{Pb}(^{48}\text{Ca}, 4n)^{252}\text{No}$ reaction (3 nb) is much lower than the value of the cross section obtained earlier [31] for this reaction (20 nb). We suppose that this over-estimation of the production cross section in the pioneer experiments with a thick target and internal beam of ^{48}Ca [31] resulted from a non-countable contribution of the $^{206}\text{Pb}(^{48}\text{Ca}, 2n)^{252}\text{No}$ reaction, which was induced due to a small admixture of ^{206}Pb in the ^{208}Pb target.

Comparing the obtained cross section values for the γ de-excitation and the $1n$ and $2n$ evaporation channels with the data on the compound nucleus cross section one could estimate relative probabilities of main compatible processes at low excitation energies. Cross section data for a symmetric component of fission [32] obtained at FLNR were used as the estimation of the compound nucleus cross section. These data are shown in the bottom panel of Fig.5.

The ratio of the cross section values gives us $\sigma_\gamma/\sigma_{fis} \simeq \Gamma_\gamma/\Gamma_f < 2 \times 10^{-5}$ at the excitation energy $E^* = (13.8 \pm 1.7)$ MeV. This estimation is much more low than the value 10^{-3} given by statistical model calculations at the same excitation energy [33]. Note that the

excitation energy is close to the position of the maximum for the giant dipole resonance cross section. A possible explanation of the discrepancy between the experimental and calculated data is connected with the approximation for the giant dipole resonance cross section used in the calculations. Probably, this approximation does not suit well for the description of the de-excitation of heavy low-excited nuclei formed in heavy ion complete fusion reactions. Nevertheless, the calculation shows a dramatic growth of the $\Gamma_\gamma/\Gamma_{tot}$ value at the excitation energy $E^* < 10$ MeV and it seems to be of interest to continue in future the same experiments at $E^* < 10$ MeV with a higher sensitivity.

For the estimation of the relative probability for neutron evaporation at a low excitation energy we used the approach developed recently for the extraction of the Γ_n/Γ_{tot} values for heavy excited nuclei [34]. Writing the expressions for the $1n$ and $2n$ evaporation channel reaction cross sections as $\sigma_{1n} = \sigma_{CN} \cdot P_{1n} \cdot G_1$ and $\sigma_{2n} = \sigma_{CN} \cdot P_{2n} \cdot G_1 \cdot G_2$, where $\sigma_{CN} \simeq \sigma_{fis}$, $P_{1n/2n}$ is the evaporation probability of a proper number of neutrons (1 or 2) at a given excitation energy and $G_{1,2} \simeq \langle \Gamma_n/\Gamma_f \rangle_{1,2}$ is the relative probability of the neutron evaporation at the first (single) or second (last) step of de-excitation, and combining them, we obtained the value of $G_1 = (4.2 \pm 1.6) \times 10^{-4}$ for the single neutron evaporation at $E^* = (16.4 \pm 1.1)$ MeV and the value of $G_2 = (2.3 \pm 0.8) \times 10^{-2}$ for the probability of the neutron evaporation at the last step of de-excitation at the most probable excitation energies of $5.9 \leq E^* \leq 13.8$ MeV. These values are much more low than the data obtained for the U and Fm CN at excitation energies of 45–70 MeV [34] and comparable with the calculated values given by statistical model considerations for the ^{256}No nucleus at low excitation energies [33].

Further comparison of the measured excitation functions for the evaporation channels and fission with the calculations based on statistical model approximations enabled us to perform some computations using the HIVAP code [35] employing the barrier penetration complete fusion model and standard statistical model approximations. Recent consideration of the reactions induced on spherical target nuclei (Pb, Bi) showed that by using HIVAP, and varying the model parameters, good agreement is achieved between the calculations and experiment for the reactions induced by the projectiles of oxygen to titanium [4]. The results of these calculations for the ^{48}Ca + ^{208}Pb reaction show rather good agreement in the case of the $2n$ channel (the upper panel of Fig. 5) and quite satisfactory results in the case of the $1n$, $3n$, $4n$ channels (the middle panel of Fig.5) and fission (the bottom panel of Fig.5). The Bass barrier [28], as an estimation of the fusion barrier position, is shown by the arrow in the bottom panel of the figure for reference. The results of calculations shown in the figure correspond to the parameters giving the best fit to the data. Those main parameters determining the fusion cross section different from the recommended ones should be mentioned here. They are: $V_o = 70$ MeV/fm and $d = 0.8$ fm (the strength and diffuseness parameters in the exponential nuclear potential) and $\sigma(r_o) = 1.8\%$ (the fluctuations of the fusion barrier expressed by means of the radius-parameter percentage). Decreasing the last-mentioned parameter, one can achieve better agreement of the calculated excitation function for the $1n$ evaporation channel, but it leads to underestimation of the fission cross section at low energies as it is shown in the figure by dashed lines

corresponding to $\sigma(r_o) = 1.5\%$. This underestimation is outside the projectile energy error bars, which are about the same for the fission cross section measurements as in the case of the described measurements for ER. The compound nucleus de-excitation was considered using the W.Reisdorf's formula for the asymptotic (macroscopic) level density parameter ($r_o = 1.153$ fm) [35] and A.V.Ignatyuk et al.'s formula for the fading influence of the ground state shell correction energy, δW_{gs}, on the level density using the damping constant $E_d = 18.5$ MeV [36]. The fit of the calculations at high excitation energies was determined by the choice of a single adjustable parameter, k_f, the scaling factor at the rotating liquid-drop fission barriers, $B_f^{LD}(L)$, which were used with the ground state shell corrections, δW_{gs}, as follows: $B_f(L) = k_f B_f^{LD}(L) - \delta W_{gs}$. In the case of the ^{208}Pb(^{48}Ca, $1n-4n$) reactions the best agreement of the calculations with the experimental data was achieved with $k_f = 0.9$. We have tested the influence of different sets of angular momenta on the results of calculations and found that restriction on an angular momentum imposed by a rotating liquid drop limit (RLDL) leads to underestimation of the fission cross section at high projectile energy and has no remarkable influence on the cross section values for ER (solid lines in the figure). This circumstance means that only small values of angular momenta contribute to the final production cross section value of ER.

5. Conclusion

The unambiguous identification of the decay chain ^{254}No $\rightarrow$ ^{250}Fm $\rightarrow$ ^{246}Cf as a result of the ^{208}Pb(^{48}Ca, $2n$) reaction, and rather good agreement of the obtained excitation function for this reaction with the results of the earlier measurements and calculations have allowed us to draw the main conclusion that the results of the first experiments at the FLNR with an intensive external beam of ^{48}Ca using the recoil separator VASSILISSA have shown the readiness of the cyclotron and separator systems for experiments aiming at production of heavy ER in ^{48}Ca-induced reactions. The high intensity of the beam and suitable background conditions for the registration and identification of α radioactivity allow performing experiments on the synthesis of the heaviest elements in complete fusion reactions between ^{48}Ca and actinide target nuclei with a sensitivity of up to a few pb and in the region of half-lives for nuclear species from a few microseconds (the time of flight through the separator) to several hours.

Acknowledgments

The authors are thankful to Dr. B.I.Pustylnik for fruitful discussions, to A.N.Shamanin and E.N.Voronkov for their help in the maintenance of VASSILISSA, and to the U-400 crew for providing a stable and intensive beam of ^{48}Ca.

This work was performed partially under the financial support of the Russian Foundation for Basic Research, contract No.96-02-17209, and the INTAS Foundation, contract No.96-662.

References

1. Smolanczuk R., Sobiczewski A. — In: Proc. of the XV Nuclear Physics Divisional Conference on Low Energy Nuclear Dynamics, April 18–22, 1995, St.Petersburg, Russia.
2. Sahm C.-C. et al. — Nucl. Phys, 1985, v.441, p.316.
3. Quint A.B. et al. — Z. Phys., 1993, v.A346, p.119.
4. Sagaidak R.N. et al. — In: Proc. of the VI International School-Seminar on Heavy Ion Physics, Sept. 22–27, 1997, Dubna, Russia, World Scientific, 1998, p.323.
5. Yeremin A.V., Utyonkov V.K., Oganessian Yu.Ts. — In: Proc. of Tours Symposium on Nuclear Physics III, September 2–5, 1997, Tours, France.
6. Oganessian Yu.Ts. — Nucleonika, 1977, v.22, p.89.
7. Hulet E.K. et al. — Phys. Rev. Lett., 1977, v.39, p.385.
8. Oganessian Yu.Ts. et al. — Nucl. Phys., 1978, v.A294, p.213.
9. Armbruster P. et al. — Phys. Rev. Lett., 1985, v.54, p.406.
10. Gikal B.N., Gulbekian G.G., Kutner V.B. — In: Proc. of 15th Int. Conf. on Cyclotrons and Their Applications, 14–19 June, 1998, Caen, France.
11. Yeremin A.V. et al. — Nucl. Instr. & Meth., 1994, v.A350, p.608.
12. Yeremin A.V. et al. — Nucl. Instr. & Meth., 1997, v.B126, p.329.
13. Gäggeler H. et al. — Nucl. Phys., 1989, v.A502, p.561c.
14. Lazarev Yu.A. et al. — Nucl. Phys., 1994, v.A580, p.113.
15. Ziegler J.F. — Computer code SRIM-97, http://www.research.ibm.com/ionbeams.
16. Andreyev A.N. et al. — Nucl. Instr. & Meth., 1995, v.A364, p.342.
17. Popeko A.G. et al. — Nucl. Instr. & Meth., 1997, v.B126, p.294.
18. Essel A.N., Richter M., Spreng W. — GOOSY, GSI report, Darmstadt, 1988.
19. Lavrentev A.Yu. — Computer code VASNEW, JINR, Dubna, 1998.
20. Firestone R.B., Shirly V.S. (editors). — Table of Isotopes, 8th edition, John Wiley & Sons, Inc., NY (1996).
21. Heßberger F.P. et al. — Z. Phys., 1997, v.A359, p.15.
22. Andreyev A.N. et al. — Z. Phys., 1993, v.A345, p.389.
23. Nitschke J.M. et al. — Nucl. Phys., 1979, v.A313, p.236.
24. Ghiorso A. et. al. — Nucl. Instr. & Meth., 1994, v.A350, p.608.
25. Münzenberg G. et al. — Z. Phys., 1981, v.A302, p.7.
26. Heßberger F.P. et al. — Z. Phys., 1985, v.A321, p.317.
27. Schmidt K.-H. et al. — Z. Phys., 1984, v.A316, p.19.
28. Bass R. — Lect. Not. Phys., 1980, v.117, p.281.
29. Gardes D. et al. — Phys. Rev., 1980, v.C21, p.2447.
30. Gardes D. et al. — Phys. Rev., 1978, v.C18, p.1298.
31. Flerov G.N. et al. — Nucl. Phys., 1976, v.A267, p.359.
32. Itkis M.G. et al. — In: Proc. of the Intern. Conf. on Structure of Nuclei under Extreme Conditions, March 31 – April 4, 1998, Padova, Italy, to be published in Nuovo Cimento, 1998.

33. Iljinov A.S., Oganessian Yu.Ts., Cherepanov E.A. — Yad. Fiz., 1981, v.33, p.997 (in Russian).
34. Sagaidak R.N. et al. — J. Phys. G: Nucl. Part. Phys, 1998, v.24, p.611.
35. Reisdorf W. — Z. Phys., 1981, v.A300, p.227.
36. Ignatyuk A.V. et al. — Yad. Fiz., 1975, v.21, p.485 (in Russian).

Received on October 30, 1998.